# Alkaline oxide interface modifiers for silicon fiber production

**Erlend F. Nordstrand,[1] Andrew N. Dibbs,[2] Andreas J. Eraker,[2] and Ursula J. Gibson[2,*]**

[1]*Department of Materials Sciences, Norwegian University of Science and Technology, 7491 Trondheim, Norway*
[2]*Department of Physics, Norwegian University of Science and Technology, 7491 Trondheim, Norway*
*[*]ursula.gibson@ntnu.no*

**Abstract:** We demonstrate the ability to pull small diameter silicon-core fibers with low oxygen content by using interface modifiers between the silica cladding and the semiconductor. Alkali earths scavenge oxygen and form a fine-structured eutectic that accommodates thermal strain and may be useful as an intermediate index cladding layer for optical applications. NaO, MgO, SrO, CaO and BaO interface modifiers were tested. CaO coated fibers were made with core diameters down to 10 microns, small bending radii, low oxygen incorporation, and optical losses below 4 dB/cm at 1.55 microns.

OCIS codes: (060.2280) Fiber design and fabrication; (060.2290) Fiber materials.

## References and links

1. J. Bei, T. M. Monro, A. Hemming, and H. Ebendorff-Heidepriem, "Fabrication of extruded fluoroindate optical fibers," Opt. Mater. Express **3**(3), 318–328 (2013).
2. M. Saad, "Indium fluoride glass fibers," Proc. SPIE **8275**, 82750D, 82750D–6 (2012).
3. A. Peacock and N. Healy, "Parabolic pulse generation in tapered silicon fibers," Opt. Lett. **35**(11), 1780–1782 (2010).
4. D.-J. Won, M. O. Ramirez, H. Kang, V. Gopalan, N. F. Baril, J. Calkins, J. V. Badding, and P. J. A. Sazio, "All-optical modulation of laser light in amorphous silicon-filled microstructured optical fibers," Appl. Phys. Lett. **91**(16), 161112 (2007).
5. L. Lagonigro, N. Healy, J. R. Sparks, N. F. Baril, P. J. A. Sazio, J. V. Badding, and A. C. Peacock, "Low loss silicon fibers for photonics applications," Appl. Phys. Lett. **96**(4), 041105 (2010).
6. B. Scott, K. Wang, V. Caluori, and G. Pickrell, "Fabrication of silicon optical fiber," Opt. Eng. **48**(10), 100501 (2009).
7. J. Ballato, T. Hawkins, P. Foy, R. Stolen, B. Kokuoz, M. Ellison, C. McMillen, J. Reppert, A. M. Rao, M. Daw, S. R. Sharma, R. Shori, O. Stafsudd, R. R. Rice, and D. R. Powers, "Silicon optical fiber," Opt. Express **16**(23), 18675–18683 (2008).
8. J. Ballato, T. Hawkins, P. Foy, B. Yazgan-Kokuoz, R. Stolen, C. McMillen, N. K. Hon, B. Jalali, and R. Rice, "Glass-clad single-crystal germanium optical fiber," Opt. Express **17**(10), 8029–8035 (2009).
9. B. L. Scott, K. Wang, and G. Pickrell, "Fabrication of n-type silicon optical fibers," IEEE Photon. Technol. Lett. **21**(24), 1798–1800 (2009).
10. T. Minami, S. Maeda, M. Higasa, and K. Kashima, "In-situ observation of bubble formation at silicon melt–silica glass interface," J. Cryst. Growth **318**(1), 196–199 (2011).
11. S. M. Schnurre and R. Schmid-Fetzer, "Reactions at the liquid silicon/silica glass interface," J. Cryst. Growth **250**(3-4), 370–381 (2003).
12. J. Ballato, T. Hawkins, P. Foy, B. Yazgan-Kokuoz, C. McMillen, L. Burka, S. Morris, R. Stolen, and R. Rice, "Advancements in semiconductor core optical fiber," Opt. Fiber Technol. **16**(6), 399–408 (2010).
13. S. Morris, T. Hawkins, P. Foy, C. McMillen, J. Fan, L. Zhu, R. Stolen, R. Rice, and J. Ballato, "Reactive molten core fabrication of silicon optical fiber," Opt. Mater. Express **1**(6), 1141–1149 (2011).
14. S. Morris, T. Hawkins, P. Foy, J. Hudson, L. Zhu, R. Stolen, R. Rice, and J. Ballato, "On loss in silicon core optical fibers," Opt. Mater. Express **2**(11), 1511–1519 (2012).
15. K. Wilm and G. Frischat, "Coating and diffusion studies to improve the performance of silica glass crucibles for the preparation of semiconducting silicon single crystals," Glass Technol. - Eur. J. Glass Sci. Technol. A **47**(1), 7–14 (2006).
16. A. Cröll, R. Lantzsch, S. Kitanov, N. Salk, F. R. Szofran, and A. Tegetmeier, "Melt-crucible wetting behavior in semiconductor melt growth systems," Cryst. Res. Technol. **38**(78), 669–675 (2003).
17. I. Brynjulfsen, A. Bakken, M. Tangstad, and L. Arnberg, "Influence of oxidation on the wetting behavior of liquid silicon on $Si_3N_4$-coated substrates," J. Cryst. Growth **312**(16-17), 2404–2410 (2010).

18. F. A. Martinsen, E. F. Nordstrand, and U. J. Gibson, "Purification of melt-spun metallurgical grade silicon micro-flakes through a multi-step segregation procedure," J. Cryst. Growth **363**, 33–39 (2013).
19. F. He, S. Zheng, and C. Chen, "The effect of calcium oxide addition on the removal of metal impurities from metallurgical-grade silicon by acid leaching," Metall. Mater. Trans., B, Process Metall. Mater. Proc. Sci. **43**(5), 1011–1018 (2012).
20. M. D. Himel and U. J. Gibson, "Measurement of planar waveguide losses using a coherent fiber bundle," Appl. Opt. **25**(23), 4413–4416 (1986).
21. M. H. Jenkins, B. S. Phillips, Y. Zhao, M. R. Holmes, H. Schmidt, and A. R. Hawkins, "Optical characterization of optofluidic waveguides using scattered light imaging," Opt. Commun. **284**(16-17), 3980–3982 (2011).
22. Lambda-Photometrics, "Model2010" http://www.lambdaphoto.co.uk/products/150.110.100.007 (2013).
23. C. W. Bale, P. Chartrand, S. A. Degterov, G. Eriksson, K. Hack, R. Ben Mahfoud, J. Melançon, A. D. Pelton, and S. Petersen, "FactSage thermochemical software and database," Calphad **26**(2), 189–228 (2002).
24. A. Cruz-Ramírez, J. Romo-Castañeda, M. Á. Hernández-Pérez, M. Vargas-Ramírez, A. Romero-Serrano, and M. Hallen-López, "An application of infrared analysis to determine the mineralogical phases formation in fluxes for thin slab casting of steel," J. Fluor. Chem. **132**(5), 323–326 (2011).
25. X. Huang, S. Koh, K. Wu, M. Chen, T. Hoshikawa, K. Hoshikawa, and S. Uda, "Reaction at the interface between Si melt and a Ba-doped silica crucible," J. Cryst. Growth **277**(1-4), 154–161 (2005).
26. D. Romero, J. M. F. Romero, and J. J. Romero, "Distribution of metal impurities in silicon wafers using imaging-mode multi-elemental laser-induced breakdown spectrometry," J. Anal. At. Spectrom. **14**(2), 199–204 (1999).
27. A. J. Eraker and U. J. Gibson (Dept. of Physics, Norwegian Univ. of Sci. and Technol., 7491 Trondheim, Norway) are preparing a manuscript to be called "Optical loss measurements in silicon fibers".

## 1. Introduction

Fiber materials for the infrared are of increasing importance as new laser sources are developed throughout the region from 1 to 10 microns. Although there has been significant development of glassy materials [1,2], silicon-core fibers have attracted particular interest due to their high index of refraction, non-linear properties [3], and potential as all-optical light modulators [4]. High-quality fibers of limited length have been fabricated by chemical vapour deposition within the pores of photonic crystal optical fibers [5].

Recently, Scott [6] and Ballato [7] published results on the use of molten core fiber-optic pulling techniques to form silicon and germanium [8] fibers encased in glass. This technique offers the promise of scale-up to industrial quantities of material. While production of many meters of germanium fiber with core diameters down to 15 microns [8] is reported, silicon fibers drawn in a fiber tower have been larger, with core diameters of 100 microns [7] and shorter. Benchtop fibers of silicon with cores down to 10 microns have been demonstrated using a powder-in tube method [6], but lengths have been limited to a few cm [9]. Gas production due to the reaction of silicon with silicon oxide [10], stress due to thermal mismatch with the glass sheath [11], and discontinuous cores can all contribute to poor performance. Significant progress has been made in assessing and improving the crystallographic quality [12] and impurity content [13] of these fibers, and in understanding the mechanisms responsible for optical losses [14].

One aspect that has so far not been investigated is the use of an intermediate layer between the silicon and the silica tube to moderate stress, remove impurities and provide a gradient index of refraction. Although there are some wetting studies of molten silicon available, they center around materials suitable as crucibles for melting [15] and directional recrystallization [16,17]. Recent studies on the use of silicon carbide for removal of oxygen [13], and purification of silicon in low-dimensional structures [18] suggested the use of a reactive species for this purpose. Choice of a suitable interface material was guided by the principles that it should be an oxide to minimize chemical complexity, it should form a eutectic with the silicon with a melting point below the softening point of the glass to reduce stress, and that the metal ion should be less electronegative than silicon to assist with oxygen scavenging from the core. Alkaline earth oxides are routinely used in the purification of silicon [19], and calcium oxide satisfies the criteria above. CaO forms hydroxides upon the addition of water, and thus an aqueous route can be used in the preparation of a preform with a layer of CaO on the inside of the silica. NaO, BaO, MgO and SrO were also investigated, with varying degrees of success; SrO and NaO, as well as NaO-BaO mixtures were least successful, resulting in

distortion of the glass-silicon interface, or large cavities in the core. CaO and CaO-MgO blends performed best, and the results presented here are on CaO. Several grades of silicon were used in these studies, as we also have interest in the segregation of impurities in limited-dimension samples [18], but the results here are limited to electronic and solar grades. In these preliminary studies, the emphasis was on the mechanical and microstructural properties. Use of higher purity starting materials can be expected to improve the optical properties of the fibers.

We present studies on the use of alkaline-earth interface modifiers to improve the mechanical properties of silicon-based fibers, demonstrating low-oxygen core content, core diameters down to 10 microns and low damage to the silica cladding, as evidenced by small bending radii. This technique should be adaptable to the production of high quality optical fibers when performed in a commercial drawing tower, particularly when employing MOCVD-deposited oxide interface modifiers.

## 2. Experimental

We prepared preforms using small diameter silica tubes (i.d. 2 mm, o.d. 4mm), with a typical length of 200mm. The ratio of the core to cladding dimensions is large, and the silica cladding of fibers prepared without the interface modifier were stressed and cracked so extensively that they disintegrated on handling, or in some cases spontaneously upon cooling.

Deionized water and CaO powder (Sigma Aldrich >99.9%) were combined in a 3:1 ratio a beaker and allowed to react, forming "milk of lime" according to the reaction

$$CaO(s) + H_2O \rightarrow Ca(OH)_2(aq) \tag{1}$$
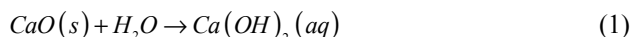
The preform tube was connected to a low-level vacuum, and the hydroxide mixture was drawn into the tube by briefly inserting the end of the tube into the liquid. This allowed us to make uniformly coated tubes, where the thickness of the coating was regulated by the viscosity of the hydroxide mix. Typical ratios of oxide to silicon were 1:8 by weight. The tubes were dried overnight at 100 °C before sealing one end using an oxy-acetylene torch. The baking dehydrates the coating and returns it to the oxide form, though reaction with atmospheric $CO_2$ may result in small quantities of calcium carbonate. Any carbonate would be decomposed at 825 °C, well below the temperature at which fiber drawing occurs. Silicon granules were prepared by crushing polysilicon or an n-type solar silicon wafer (Norsun, nominal 7N purity base material) in a mortar and pestle to a size of approximately 0.5 mm or less. The coated preform was then filled with this powder.

The preforms were held vertically, and heated using an oxyacetylene flame centered above the bottom of the preform until melting of the silicon was observed. Further heating was applied to soften the silica. The high temperature flame precluded measurement of the draw temperature. The bottom of the tube was then pulled down at speeds of 60-150 meters per minute, resulting in fibers of up to 450 mm in length, limited by the vertical clearance of our setup. Fibers drawn with or without vacuum application during the pull showed no significant differences, and results presented here are for fibers drawn in air.

Analysis of the fibers was performed using x-ray fluorescence microprobe with wavelength and energy dispersive spectrometers, scanning electron microscopy, Raman spectroscopy (Horiba LabRam HR800-UV) and UV photoluminescence spectroscopy. An excimer laser operating at 248 nm was used as the UV excitation source, and an Avantis Avaspec ULS2048 spectrometer was used to acquire the optical data. Cross-sectional samples were prepared by mechanical polishing; these were used for microprobe and Raman characterization.

Optical waveguide loss measurements were made by collecting the scattered light as a function of distance along the bare silicon core [20–22]. The scatter method allowed us to make measurements insensitive to variations in the input coupling. We used a modulated 5 mW fiber-coupled laser diode operating at 1.55 microns, an amplified Ge detector (ThorLabs

PDA30B) and a lock-in amplifier. For most measurements, the silicon fiber was mounted inside a commercial fiber optic ferrule, and a ferrule coupler then aligned it with the output fiber of the laser. The silica and CaO were removed by HF etching prior to measurements, to eliminate cladding modes, and a pickup fiber was scanned along the waveguide to collect the scattered light for a determination of the fiber losses. Figure 1 shows this setup. Measurements made with a GRIN lens collimator and a 10x objective mounted in an x-y translator for coupling into the fiber yielded similar results.
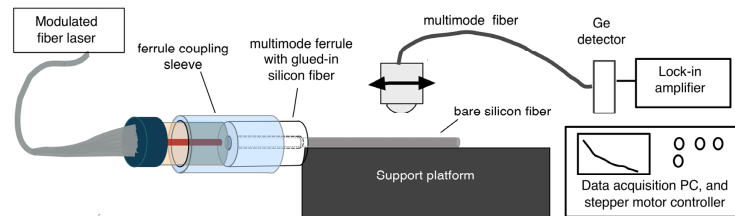


Fig. 1. Schematic of butt-coupling and scanning fiber arrangement.

Multiple measurements of an individual fiber are highly reproducible (e.g. with 10 measurements, the mean loss was 4.365 with a standard deviation of 0.0243 and a coefficient of determination ($R^2$) of >.972 for all the fitted curves). Intentionally tilting the fiber scanning stage by 1 degree or defocussing the pickup lens by 60% percent of its focal length resulted in less than 5% change in the fitted value. Rotating the fiber around its axis did not lead to a measurable change in the derived loss value.

Scanning electron microscopy of the fiber surface after etching was performed in a Hitachi TM-3000 tabletop SEM.

## 3. Results and discussion

Figure 2(a) shows a scanning electron micrograph of the cross-section of one of the fibers drawn from metallurgical grade silicon using CaO as an interface modifier, Fig. 2(b) is a microprobe scan across the interface from top to bottom, and Fig. 2(c) is a Raman spectrum from the core.
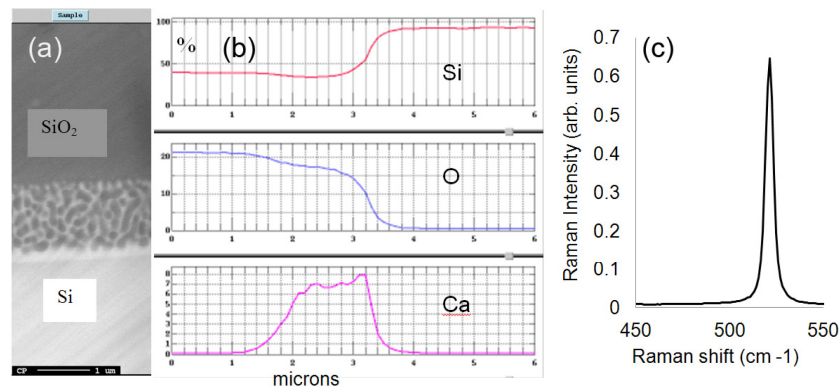


Fig. 2. (a) SEM image (scale bar is 1µm) (b) microprobe data from a line scan from the cladding to the core. The interface modifier makes a layer about one micron thick, with good confinement of calcium to the layer. Oxygen in the silicon core is at the limit of detection. (c) Si Raman signal from a fiber core.

Although the absolute percentages of the components have not been calibrated for the microprobe data on this system, the relative amounts can be used to interpret the results.

The calcium is localized at the interface, the silicon content tapers off as the eutectic microstructure takes over. There is a small drop in the silicon content in the interface region, relative to the amount in the silica cladding; this correlates with the presence of Ca. The oxygen content is reduced in the interface region, showing that the region is a mixture of semiconductor and oxide; this demonstrates that the index of refraction of this region will be intermediate between that of the core and cladding. The oxygen content in the silicon core is at the detection limit of the technique. This is in contrast to the initial results of Ballato et al [7], and comparable to the results that they achieved with silicon carbide used to scavenge oxygen [13]. The 100-300 nm grain size of the eutectic microstructure is typical for this composition and drawing condition, and represents a potential challenge for transmission of short wavelengths as it may introduce scatter. In the 3-5 micron region where these fibers might be most useful, this will be less problematic. Preliminary results on binary mixtures of alkaline earth oxides (MgOH and CaO) suggest that this structure is finer the presence of an additional oxide, most likely due to increased nucleation, as the MgO-rich phases will precipitate out at higher temperatures, seeding the solidification of the Ca-rich phase. The Raman results in Fig. 2(c), with a strong peak at 520 $cm^{-1}$, and no signal at 480 $cm^{-1}$ demonstrate that the core is crystalline silicon, with little or no amorphous component.

Figure 3 shows the phase diagram for $CaO-SiO_2$ [23]. We believe that the eutectic present at 1437 °C is responsible for the superior drawing properties of fibers made with this interface
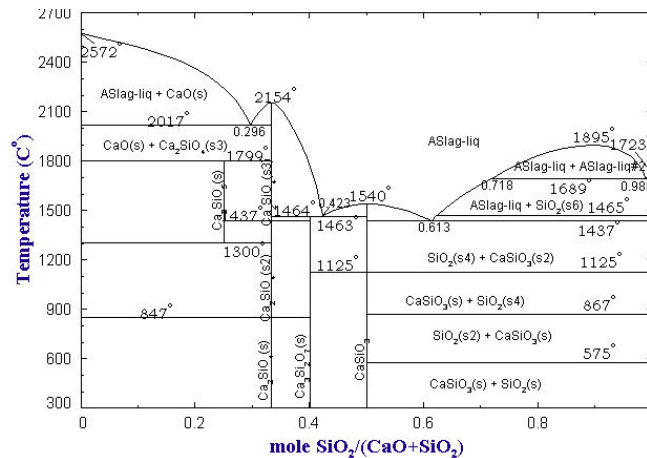


Fig. 3. Phase diagram of the CaO – $SiO_2$ system [23].

modifier. A lower-viscosity liquid forms at the interface between the silica glass and the molten silicon, allowing differential contraction. The silicon and the silicate phase separate, and we have not observed silicate inclusions in the fiber core with CaO, even when starting with a mixture of silicon and CaO powders. This suggests that the silicates preferentially wet the preform walls. Although the eutectic forms at a temperature slightly above the silicon melting point in the pure oxide system, it is likely that this temperature is suppressed in the presence of liquid silicon. The oxides are expected to separate into a mixture of wollastonite ($CaSiO_3$) and $SiO_2$ upon cooling. Wollastonite is a byproduct in silicon slag refining, and is used as a flux for low-temperature steel manufacturing [24]. It is known to be an effective sink for impurities in silicon, and the lower electronegativity of calcium relative to silicon explains the oxygen scavenging that we observe. Related studies on silica crucibles coated with BaO decreased erosion of the silica glass by molten silicon, in the presence of the coating, although there are conflicting interpretations of the mechanism [15,25].

Figure 4(a) presents an SEM image, showing the small core sizes possible. This fiber end was fractured, and shows damage due to that process. Figure 4(b) shows the bending radius
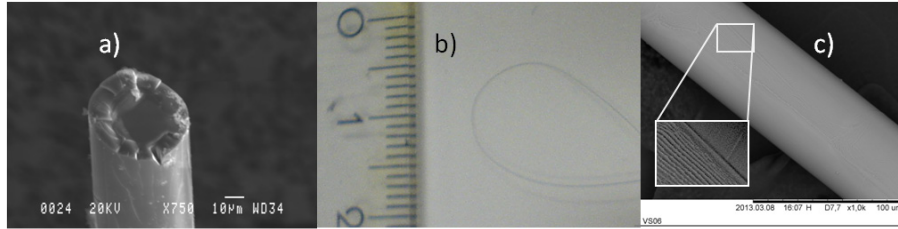


Fig. 4. (a) Fractured small-diameter fiber, (b) bending radius of the fiber shown in the first panel (ruled markings are cm) (c) SEM image of the surface of a ~65 μm diameter fiber, used for waveguide loss measurements, after removal of the glass coating. Striations shown in the expanded and contrast-enhanced inset likely arise from the eutectic decomposition of the oxides.

achieved with small fibers, and Fig. 4(c) shows a bare silicon core; close inspection shows striations with a periodicity of ~100nm along the surface.

Shown in Fig. 5 are fluorescence results obtained with excitation at 248nm for a bare silica tube, calcium oxide powder, and fibers prepared with CaO at the interface. The bulk of the emission is due to the silica cladding, but peaks that are not accounted for by either the silica cladding or CaO appear at 300 and 670 nm.
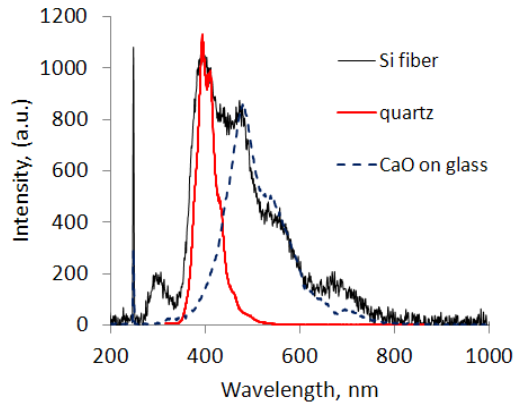


Fig. 5. Fluorescence spectrum of fibers, empty silica tubing, and CaO slurry after drying.

The shoulder at 500 nm is thought to be calcium carbonate, and the peak at 300 is due to silicon [26]. Calcium silicate is not expected to fluoresce in the visible, except in the presence of impurities. As the purity of our calcium oxide powder was only 99.9%, the peak at 670 is likely due to impurity inclusion in the nanocrystalline host in configurations that allow optical emission. It is also possible that impurities removed from the silicon melt contribute to this signal.

Measured losses on bare silicon fiber cores from different preforms varied from 3.8dB/cm to over 20dB/cm, depending on the surface quality of the fiber (which is a function of the interface layer thickness and drawing parameters), and the type of silicon used. The sample shown in Fig. 4(c), made from the Norsun material, had losses of approximately 3.8dB/cm, measured over a 1 cm length; all fibers from this material had losses less than or equal to 11dB/cm; secondary ion mass spectroscopy will be performed [27] to determine the impurity levels in the different silicon materials. However, loss measurements were influenced by areas with high scatter; in fibers with higher losses, the scatter could be correlated with core-surface

features observed in the microscope. Thicker interface layers appeared to be associated with hydrodynamic instabilities that were responsible for the surface roughness of the cores. Measurements of the throughput yielded comparable values for the loss, despite poor end face quality, which leads us to believe that reduced losses will be observed in smoother fibers, and those dominated by lower order modes, where the field is more confined to the core.

## 4. Conclusions

We demonstrate the ability to pull small diameter silicon fibers with good flexibility when using an interface modifier to scavenge oxygen from the core, relieve thermal mismatch, and decrease the viscosity of the boundary between the molten silicon and the silica glass. Alkaline earth oxides, particularly CaO and MgO lead to formation of fibers with reduced core voids, high quality interfaces and superior mechanical properties. Introduction of interface modifiers in preforms made by MOCVD, and the use of a commercial drawing tower may be expected to result in material with improved uniformity and lower losses.

## Acknowledgments